

## ANALYSIS OF A NACA 0012 PROFILE IN A SMALL SUBSONIC INDUCTION DRIVEN WIND TUNNEL

Ariane Fassina Bredariol, [aribreda@hotmail.com](mailto:aribreda@hotmail.com)

Universidade de Taubaté, Rua Daniel Danelli s/n, Jardim Morumbi, CEP: 12060-440, Taubaté – SP

Alcides Rocha da Silva, [alcidesars@iae.cta.br](mailto:alcidesars@iae.cta.br)

João Batista Pessoa Falcão Filho, [jb.falcao@ig.com.br](mailto:jb.falcao@ig.com.br)

Instituto de Aeronáutica e Espaço (IAE), Divisão de Aerodinâmica (ALA), Pça. Marechal Eduardo Gomes, 50  
CEP: 12228-904, São José dos Campos - SP

**Abstract.** *The Aerodynamic Division (ALA) from the Institute of Aeronautics and Space (IAE) has recently developed a small wind tunnel driven by induction. Through a test campaign, it was verified the good quality of the flow in the test section, certifying it to perform reliable tests. The tunnel is driven by a mixing chamber which uses a supersonic injector working at Mach number 1.9. As the stagnation pressure varies in the injector up to 10 bar, the flow in the test section is established up to Mach number 0.37. The test section is square with side length of 0.144 m. In these kinds of installations, it is very common to use standard devices to investigate the quality of the flow in the test section, such as Pitot probes, pressure probes, yaw-meters, etc. In addition, standard models with simple geometries are frequently used in order to compare the experimental results with theoretical predictions and even with experimental results from other wind tunnels. Tests like these characterize a specific phase nominated calibration phase, in which the main operational characteristics of the installation are assessed. With this aim, an aeronautical profile NACA 0012 was installed in the small wind tunnel, since there are extensive available data in the scientific literature. Pressure taps over the profile surface were done and they were connected to pressure sensors to determine the pressure distribution over the model. Two models with 10,4% and 7% of blockage ratio were installed in the test section, and the installation allows angle of attack adjustments. Near the test section entrance, a pressure tap at the tunnel wall was used to determine the undisturbed Mach number condition. This report describes the main steps undertaken during the test campaign with the NACA 0012 models in the small wind tunnel in the range from Mach number 0.15 to 0.37 and angles of attack -5, 0 and +5, with concern about the blockage effects.*

**Keywords:** *subsonic wind tunnel, profile NACA 0012, pressure coefficient*

### 1. INTRODUCTION

The Aerodynamic Division (ALA) from the Institute of Aeronautics and Space (IAE) recently developed a mixing supersonic/subsonic chamber, it is operated by a supersonic injector working in choked condition at Mach number 1.9 to do research of mixing jets and optimize some of the mixing chamber geometric parameters (injector angle and the angle in diffuser walls) and operation (stagnation pressure at the injector). The mixing chamber uses the compressed air system existent in the TTP (Pilot Transonic Wind Tunnel) that allows the automatic control of the pressure at the injector and, consequently of the inducted mass flow from the ambient. These kinds of installations are very useful, in which a small mass flow with high speed can accelerate a big mass flow with low speed. Later, this installation received a squared test section with side of 0.144 m, and its operation is guaranteed by the mixing chamber that induces the flow from the environment until the desired Mach number at the test section is established. Figure 1 shows the installation of this small wind tunnel, in which the maximum Mach number achieved was 0.37. The installation was verified about the operational characteristics (time of response, Mach number control, etc.) and about the flow quality, by determining the uniformity of the flow in test section, through a spatial sweep using Pitot probes set connected to a two-dimensional positioner (Faria, 2011). In the figure it is possible to observe the main elements of the small tunnel: (1) the collector with geometry change, from circular to square, (2) the squared test section with 0.144 m of side and 0.50 m of length and with 3 windows for visualization, (3) the injector with fixed geometry which operates choked at Mach number 1.9 and with rectangular exit section of 0.023 m by 0.016 m, (4) the mixing chamber with width of 0.173 m, height of 0.228 m and length of 0.685 m and (5) the diffuser with length of 1.725 m, and with superior and inferior articulated walls to allow angle adjustments from 0.8° to 8°.

The small tunnel operation is done by keeping air from the injection system of TTP (Goffert *et al.*, 2008). Figure 2 shows a numbered diagram with the main components of generation and control systems of compressed air. Two piston compressors with 3 stages and 92 kW of power each (1) load two reservoirs with high pressure with 10 m<sup>3</sup> of capacity each (2). Then, the air is discharged trough a blockage security valve (3) and a pressure controller valve (4), and its opening position is modulated by a pressure signal desired at the injector chamber (6). The control valve automatically

regulates the pressure in the tubing of the injector by a program developed in LabView© – the injector can work with pressures up to 10 bar and it operates choked with Mach number of 1.9. This way the injector discharges a stable mass flow in the mixing chamber (7) that later is discharged in the diffuser and then to the environment. The low pressure created in the mixing chamber and the transfer of momentum quantity between the inducer and induced flow guarantee a continuous suction from the environment to inside the test section of the small tunnel (9). The item (5) is a safe valve that burst a protective disk if the pressure in the injector exceeds 16 bar.

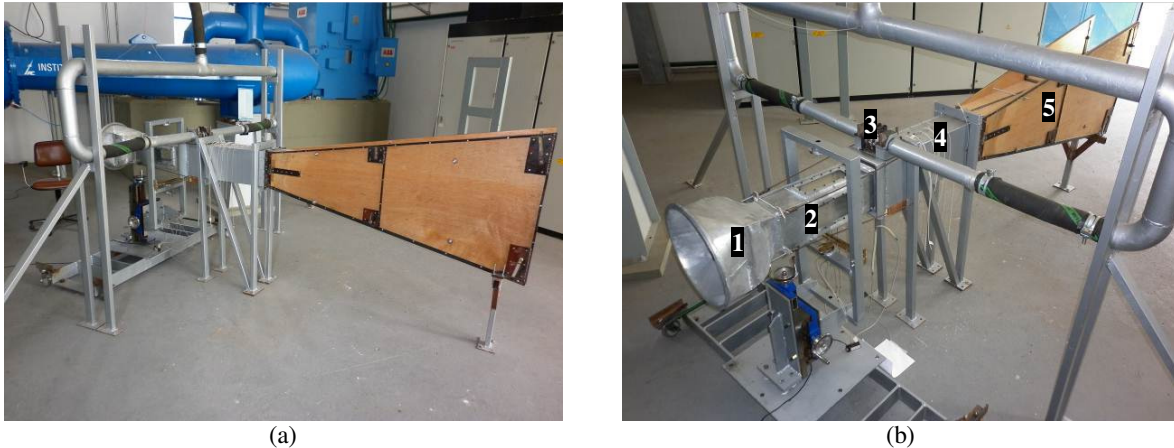


**Figure 1. Views of the installation of the small tunnel of ALA: (a) in the first plan the diffuser, (b) in the first plan the inlet collector and the Pitot probes mounting device.**

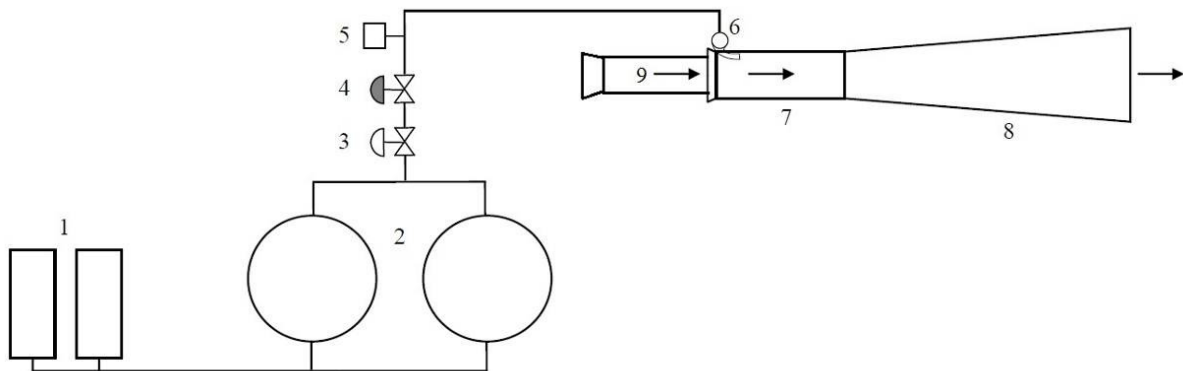


**Figure 2. Diagram of the configuration of the generating compressed air system to the small tunnel.**

The installation of any wind tunnel has a calibration phase, in which all the functionality are verified and finally an operational map is raised. Still in this phase, the flow conditions in the test section are investigated for uniformity and stability to better mimic the flight conditions. Finally, some typical models, those whose aerodynamic behavior is much documented, are tested to certify that the tunnel gets results with the desired accuracy. Among several options usually used, the symmetrical profile NACA 0012 stands out because of its vast literature that reports theoretical, numeric and experimental results in several wind tunnels and at several speed regimes.

The profile NACA 0012 was developed in 1932 by NACA (“National Advisory Committee for Aeronautics”) with a series known as NACA 4 digits. The numeration system to these airfoils is based on its geometry. The first digit indicates the maximum value of the ordinate  $y$  from the midline in percentage of the chord; the second digit is the distance from the leading edge to the maximum point of camber in tenths of the chord. The two final digits indicate the thickness of the airfoil in percentage of the chord. The NACA 0012 profile is symmetric, with maximum thickness of 12% in relation to the chord, and it can be expressed by the equation (Menezes, 1994)

$$\frac{y}{c} = \frac{t}{c} \left[ a_0 \sqrt{\frac{x}{c}} + a_1 \left( \frac{x}{c} \right) + a_2 \left( \frac{x}{c} \right)^2 + a_3 \left( \frac{x}{c} \right)^3 + a_4 \left( \frac{x}{c} \right)^4 \right], \quad (1)$$

where  $t$  is the maximum thickness,  $c$  is the chord and the constants are:  $a_0= 1.4779155$ ,  $a_1= -0.624424$ ,  $a_2= 1.727016$ ,  $a_3= 1.3840870$  and  $a_4= -0.489769$ .

The profile was done in Aluminum and it was machined in CNC to obtain a perfect representation of its geometry. Initially a NACA 0012 profile with nine pressure taps, 0.125 m of chord and maximum thickness of 0.015 m, representing a maximum blockage ratio of 10.4% was installed in vertical direction in the test section. It was necessary to adapt the tunnel upper window so the profile could fit crossing it, as shown in Fig. 3 (a). The red arrow in the picture indicates the flow direction in the tunnel and the red point is the approximated position of a take of pressure to measure the static pressure of the non-disturbed condition, on the lateral wall of the tunnel, near the test section inlet (indicated by the white arrow). Lately another profile was available and it was installed in horizontal direction in the test section. It represents 7% of blockage ratio and it has five pressure taps, chord of 0.083 m, maximum thickness of 0.010 m, and wingspan of 0.250 m, and the installation is shown in Fig. 3(b).

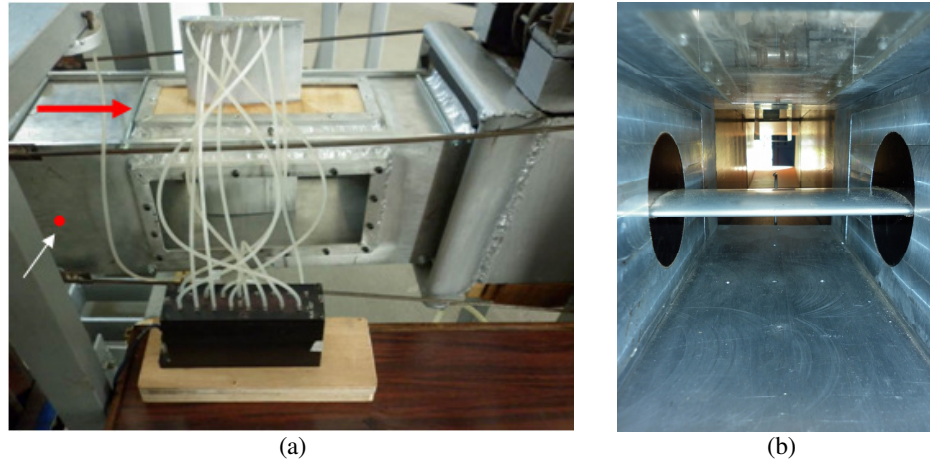


**Figure 3. View of the test section of the small tunnel: (a) with the profile NACA 0012 with blockage ratio of 10.4% installed and with the hoses connected to a pressure scanner, and (b) with the profile NACA 0012 with blockage ratio of 7% installed in horizontal direction.**

In both models, the pressure taps were machined with 0.5 mm of diameter perpendicularly to the surface of the profile, distributed along the chord direction. In Fig. 3 (a), it is seen the pressure scanner with 16 channels, model ESP-16BP from Esterline pressure Systems (PSI, 2000) that does a sweep each second and it is managed by a computer code developed in LabView©. All the channels measure differential pressure in relation to the ambient pressure. The ambient pressure is read by a reference absolute pressure gauge model 05605273, with accuracy of +/- 10 Pa, of the company TESTO do Brasil (Testo, 2000). This way, the static pressure  $p$  at each reading point is obtained by

$$p = p_{amb} + \Delta p, \quad (2)$$

where  $p_{amb}$  is the ambient pressure and  $\Delta p$  is the pressure value read by the scanner.

The pressure tap were located in only one side of the profile. So, as the profile NACA 0012 is symmetric, in order to obtain the pressure distribution in the lower and upper surfaces, with the profile at a determined angle of attack it is possible to simply turn the profile at the same angle, to have the results in the other side. This was obtained reversing the wood window frame of Fig. 3 (a) or just turning the profile of Fig. 3 (b).

## 2. PARAMETERS OF INTEREST

The most significant parameter to perform analysis with tests in airfoils is the dimensionless parameter called pressure coefficient, defined by (Anderson, 1984)

$$c_p = \frac{p - p_\infty}{q}, \quad (3)$$

where  $p$  is the local pressure on the airfoil,  $p_\infty$  is the non-disturbed flow pressure, here initially attributed to the flow condition at the test section entrance, and  $q$  is the dynamic pressure, defined by (Anderson, 1984)

$$q = \frac{1}{2} \rho_\infty V_\infty^2, \quad (4)$$

where  $\rho_\infty$  is the specific mass and  $V_\infty$  is the speed, both related to non-disturbed flow condition. From Eqs. (3) and (4) and the expressions of perfect gas equation ( $p_\infty = \rho_\infty RT_\infty$ ), the speed of sound ( $a_\infty = \sqrt{\gamma RT_\infty}$ ) and the definition of Mach number ( $M_\infty = V_\infty/a_\infty$ ), all related to the non-disturbed condition, where  $R$  is the gas constant and  $\gamma$  is the relation between specific heat at constant pressure and at constant volume, it is possible to obtain a more practical recursive equation to calculate the pressure coefficient, which is

$$c_p = \frac{\frac{p}{p_\infty} - 1}{\frac{\gamma}{2} M_\infty^2}, \quad (5)$$

where the Mach number of the non-disturbed flow is obtained using the values of total and static pressure of the non-disturbed flow, in an expression obtained from the isentropic relation (Anderson 1984):

$$M = \sqrt{\frac{2}{\gamma - 1} \left[ \left( \frac{p_0}{p_\infty} \right)^{\frac{\gamma - 1}{\gamma}} - 1 \right]}. \quad (6)$$

Initially the pressure of the non-disturbed flow was obtained by a static pressure tap near to the entrance of the test section (see Fig. 3) and the total pressure was obtained by the value of the ambient atmospheric pressure – the atmospheric acts like a big reservoir, supplying the necessary flow to the installation, when operated by injector induction. More details can be found in Silva *et al.* (2011).

#### Correction of the pressure

Every object confined to be tested in a wind tunnel suffers the action of several factors. Among them, one with most impact is the presence of the walls that can change the results if compared to a flow in a free flight. Figure 4 illustrates this fact. Considering the same conditions upstream of the wing for two different boundary conditions, (a) free flow and (b) solid walls in a wind tunnel, the flow field shows different behaviors. And they are still different from the flow condition in an open test section wind tunnel, but this is not the subject of this study. In a confined flow (Fig. 4 (b)) the streamlines are not so dislocated as in the free flight condition (Fig. 4 (a)) (Goethert, 2007). This is also true for centrifugal force intensity and pressure gradients. Another interesting fact is that in the subsonic regime the flow is accelerated by the blockage effect caused by the presence of the body: this generates pressure error reading.

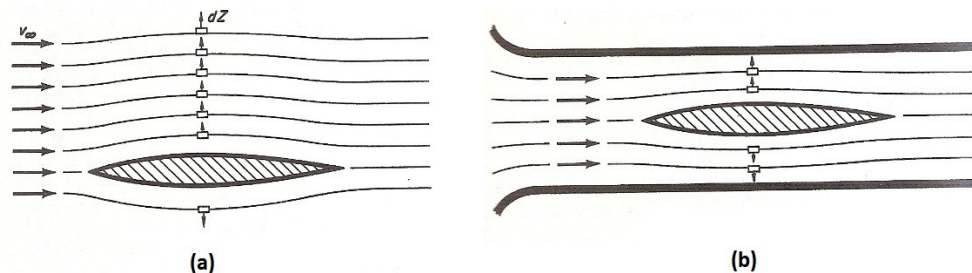


**Figure 4. Illustration of the effect caused in the flow streamlines by an airfoil: (a) in free flight, and (b) confined in a wind tunnel with solid walls.**

There are a lot of factors that affect the measures in a wind tunnel like, for example, the growth of the boundary layer that also causes a decrease of the area of passage and the downwash that is related to the distortion that the field flow suffers due to the presence of the model. During the whole useful life of a wind tunnel it is always objective to develop techniques to evaluate and correct all these effects. The present work will give attention to the most primary effect that is the blockage ratio. The presence of the model in the test section reduces the effective area. By continuity and Bernoulli equation, the air speed must rise when passing through the model, rising the aerodynamics efforts at a certain angle of attack.

It is possible to imagine a correction in the pressure readings considering only the local blockage ratio, defined by the relation between the transversal area of the model in a certain point ( $A_M$ ) and the transversal area of the test section ( $A_{ST}$ ),

$$R_B = \frac{A_M}{A_{ST}}. \quad (7)$$

From the definition equation of NACA series it is possible to determine the blockage ratio over the profile, which is given by

$$R_B = 2 \frac{T}{H} \left[ a_0 \sqrt{\frac{x}{c}} + a_1 \left( \frac{x}{c} \right) + a_2 \left( \frac{x}{c} \right)^2 + a_3 \left( \frac{x}{c} \right)^3 + a_4 \left( \frac{x}{c} \right)^4 \right], \quad (8)$$

where  $T$  is the thickness of the airfoil and  $H$  is the height of the test section and the other parameters as defined in Eq. (1). By a simple analysis, considering the incompressible flow it is possible to obtain the value of corrected pressure in function of the blockage ratio (Zucker and Biblarz, 2002)

$$p_c = p + \frac{\gamma}{2} p_\infty M_\infty^2 \left[ \left( \frac{1}{1-R_B} \right)^2 - 1 \right], \quad (9)$$

where  $p$  is the pressure in a certain point over the airfoil.

#### **Blockage effects**

There exists an interference effect associated with the fact that the model and its wake occupy a certain volume within the finite tunnel stream. The solid blockage is a function of the model thickness distribution and the ratio of the model size to the tunnel area. Any real body without the boundary layer control has a wake behind it, the effect of the wake blockage is proportional to the wake size and thus to the measured drag force on the model. The blockage factor  $\mathcal{E}_B$  can be expressed by (Garner *et al.*, 1966),

$$\mathcal{E}_B = \mathcal{E}_S + \mathcal{E}_W \quad (10)$$

where  $\mathcal{E}_S$  is solid blockage factor and  $\mathcal{E}_W$  is the wake blockage factor. The solid blockage factor  $\mathcal{E}_S$  in incompressible flow is given by

$$\mathcal{E}_S = \frac{\Delta U_S}{U} = \frac{\Pi^2}{12} \left( \frac{c}{h} \right)^2 \left( \frac{t}{c} \right)^2 \lambda_2 \quad (11)$$

where  $c$  is the chord,  $t$  the maximum thickness,  $h$  the height of the tunnel test section and  $\lambda_2$  is the shape parameter of the airfoil. The wake blockage factor  $\mathcal{E}_W$  of a two-dimensional airfoil in incompressible flow can be represented by

$$\mathcal{E}_W = \eta \left( \frac{t}{c} \right) \left( \frac{c}{h} \right) \quad (12)$$

where  $\eta$  is the Glauert's two dimensional wake-blockage factor.

The correction on the pressure coefficient  $c_p$  on the body will also be necessary because of the changes in both static and kinetic pressures of the tunnel stream. The needed correction may be written as (Garner *et al.*, 1966),

$$\Delta c_p = \frac{p - (p_\infty + \Delta p_\infty)}{\frac{1}{2} \rho U^2 + \Delta \left( \frac{1}{2} \rho U^2 \right)} = \left[ 2 - (2 - M^2) c_p \right] \mathcal{E}_B \quad (13)$$

Such an expression assumes that the observed pressures are those which would be obtained in the corrected free-air conditions.

### Pressure drop

It is possible to imagine a correction of pressure to each point of the chord along the profile; so with this objective, the profile NACA 0012 was removed of the test section. It was done a sweep only with Pitot probes, and it was possible to verify a pressure difference between the non-disturbed flow (at the inlet) and at the place where the profile would be installed. Table 1 shows the results and suggests a correction for the value of  $p_\infty$ . The pressure applied in the injector is  $p_{0,inj}$  (1 bar =  $10^5$  Pa).

**Table 1. Suggestion of free stream static pressure correction.**

$p_{0,inj}$ (bar)	Mach	$\Delta p_\infty$ (Pa)	Standard Deviation (Pa)
4	0.1920	257	38
6	0.2492	418	48
8	0.2904	620	68
10	0.3321	770	72

According to Table 1 it is possible to obtain

$$\Delta p_\infty = 1.1136x - 10722 \quad (14)$$

where  $x$  is the distance in meters between the inlet pressure reading and the point considered over de profile surface and  $\Delta p_\infty$  is the correction in Pa in the pressure read.

### Number of Reynolds effects

The number of Reynolds is a parameter of great importance to the analysis of problems in scales and it indicates the condition of the kind of the flow, laminar or turbulent, over surfaces. It can be expressed by

$$Re = \frac{\rho V \ell}{\mu}, \quad (15)$$

where  $\rho$  is the specific mass,  $V$  is the speed,  $\ell$  a parameter characteristic of the length and  $\mu$  the dynamic viscosity.

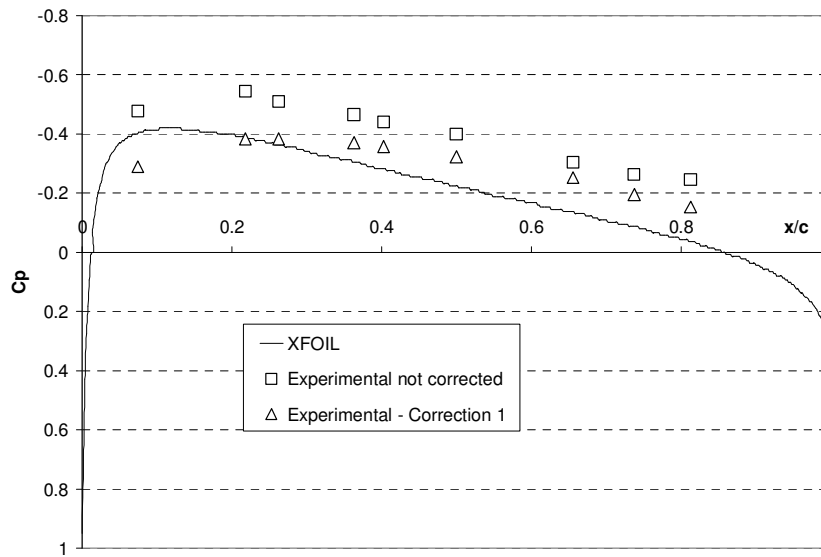
### Theoretical solution comparison

The experimental results are compared with the theoretical results obtained with the computational program XFOIL version 6.94© 2000, developed by Mark Drela from MIT and Harold Youngren from Aircraft Inc. (Drela and Youngren, 2012). The XFOIL© is an interactive program developed in FORTRAN to project and analyze of airfoils isolated at subsonic regime. The program was basically used to survey the  $c_p$  (pressure coefficient) curves on the airfoil. For the considered Mach number range (low subsonic) it is expected reliable values by using the XFOIL©.

## 3. RESULTS

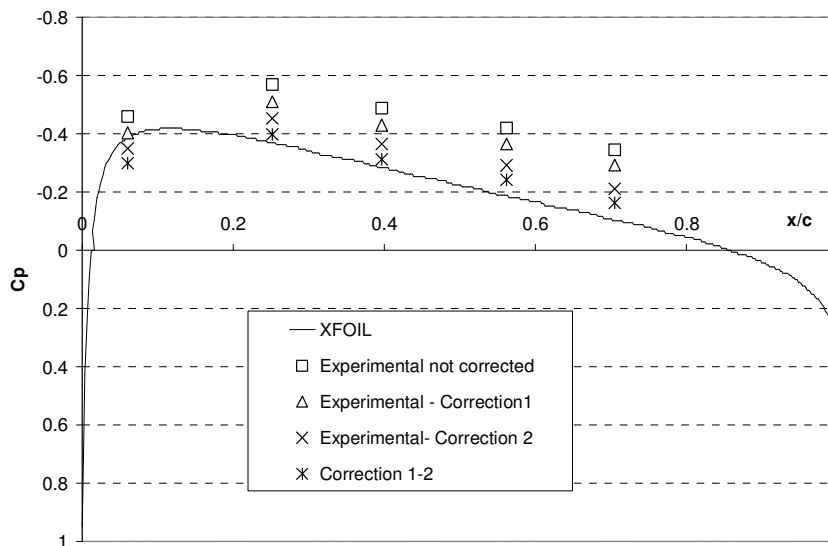
It was done 12 runs, changing the angle of attack in the profile in  $-5^\circ$ ,  $0^\circ$  and  $+5^\circ$ . To each attitude it was selected pressures of 4 bar, 6 bar, 8 bar and 10 bar in the injection control system. The runs lasted about 50 seconds and all the parameters of the control system were registered each second. First it was possible to notice that the presence of the profile at the test section with 10.4% of blockage ratio provoked a little decrease at maximum Mach number – from 0.37 to 0.345. It was possible to see, in general, that the accuracy at the control system get worse with the increase of the pressure at the injector. For the sake of brevity only some important results will be presented.

Figure 5 shows the result of the pressure distribution corresponding to the first run with Mach number 0.186 at the non-disturbed flow condition, comparing the theoretical result obtained by the program XFOIL© with the result with blockage correction. The abscissa axis registers the value along chord made dimensionless by the chord length. The results indicate that the blockage ratio of the airfoil of 10.4% seems to be excessive to be used in the test section. The maximum deviation of  $c_p$  observed with the initial data obtained related to the theoretical solution was 0.20, and with the data with correction this maximum deviation was 0.11. Although the analysis indicates that the correction procedure improved the final result, the error is still high.



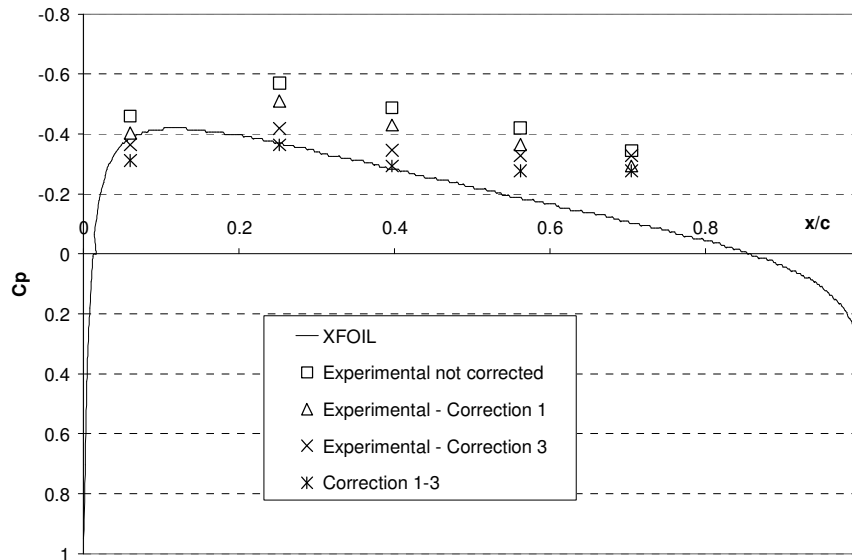
**Figure 5. Distribution of  $c_p$  of the run corresponding to the Mach number 0.186 and angle of attack zero profile with blockage ratio of 10.4%.**

Due to the unsatisfactory results with this first model, it was performed runs with the profile with 7% blockage ratio and with new corrections applied. The runs were done at  $0^\circ$  of angle of attack. It was selected pressures of 4 bar, 6 bar, 8 bar and 10 bar in the injection control system. Before these runs, to certify that the measure of the static pressure was correct; it was increased (from 1 to 5) the quantity of tap pressures to measure the static pressure of the non-disturbed flow at other measuring points at the inlet of the test section. It were done 8 runs with the new profile (7% of blockage ratio), they were done at  $0^\circ$  of angle of attack. The pressure at the injection control system was 4, 6, 8 and 10 bar. To certify the profile was aligned with the flow direction runs were done with the profile in both sides, with the pressures taps facing up and down the test section; the results were very satisfactory. Figure 6 shows the result for the profile with 7% of blockage ratio. The Mach number reached was 0.181 and the pressure applied in the injection system was 4 bar. The theoretical results were compared with the XFOIL and with the result with two different corrections. The correction 1 is according to Eq. (13) and the correction 2 is according to Eq. (14). Both corrections applied together is nominated 1-2. It is important to notice that the experimental results without correction are not good and that is very important to apply the right corrections.



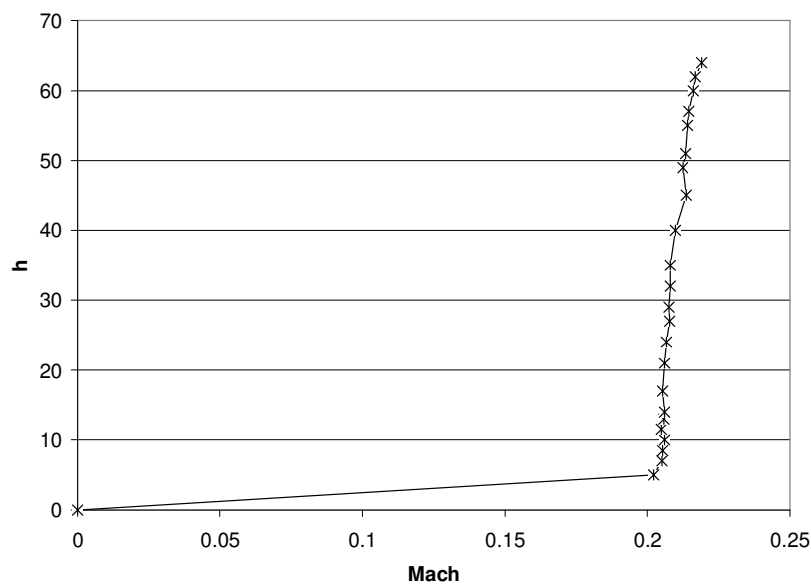
**Figure 6. Distribution of  $c_p$  on the profile with 7% of blockage ratio. The Mach number correspondent to this run is 0.181 and angle of attack zero. Corrections 1, 2 and 1-2 are shown here.**

Figure 7 shows the results to the same conditions of Fig. 6 but with some different corrections. In Fig. 7 the correction 1 is the same as in Fig. 6 and it is according to Eq. (13), the correction 3 is according to Eq. 9. Then, when correction 1 and 3 are applied together the result is the correction 1-3. By the simple analysis of the graphics is possible to realize that the correction 1-2 is the closest to the XFOIL© results. Also it is possible to note that the first point is decreasing, while the others tend to be adjusted to the curve desired.



**Figure 7. Distribution of  $c_p$  to the profile with 7% of blockage ratio. The Mach number correspondent to this run is 0.181 and angle of attack zero. Corrections 1 and 3 are shown here.**

Later, in order to investigate if the boundary layer was interfering in the results; it was done a sweep with a Pitot probe positioned between the profile and the wall of the test section. This way, it was done 23 runs (Fig. 8), and one can see that the boundary layer thickness is less than about 7 mm, and it is too small to impact in the results of  $c_p$ . The abscissas axis represents the number of Mach and the ordinates represent the distance between the Pitot probe and the test section wall ( $h$ ). It is necessary to say that the Pitot probe used was not the best one to analyze the boundary layer, but it was enough to see that the boundary layer is too small to interfere in the test results.



**Figure 8. Results of the vertical sweep done in order to investigate the boundary layer.**



#### 4. CONCLUSION

The main steps undertaken to test the NACA 0012 profile in the small induction driven tunnel of IAE were described, pointing the used devices and the profile characteristics. Initially a 10.4% blockage area model was tested and some blockage correction was presented.

In order to calibrate the small tunnel, it was tested two NACA 0012 profiles with blockage ratio of 10.4% and 7%, the results were compared with the ones obtained in numerical computation from XFOIL and with the corrected results considering the wall effect and pressure drop. It was used empirical methods of correction found in literature and developed during this work, with which it was obtained an improvement in convergence. Beyond that, it is desirable equipments with a better precision to the pressure reading. Although some procedures for correction resulted in a reasonable agreement both profiles seems to have excessive blockage ratio. Other tests with smaller model are very desirable.

#### 5. ACKNOWLEDGEMENTS

The authors thanks to IAE (Instituto de Aeronáutica e Espaço), by the viability of this work, and to CNPq – for the financial support: PIBIC and DTI process number 384448/2011-9.

#### 6. REFERENCES

- Anderson, J. D. J, 1984, *Fundamentals of Aerodynamics*, McGraw-Hill, Inc.
- Drela, M., Youngren, H., 2012, “XFOIL Subsonic Airfoil Development System,” internet site: <http://web.mit.edu/drela/Public/web/xfoil/>.
- Faria, A. F., 2011, “Desenvolvimento de uma Seção de Testes para um Mini Túnel de Vento,” Thesis of Bachelor (In portuguese), Faculdade de Tecnologia de São José dos Campos – FATEC.
- Garner, H. C., Rogers, W. E., Acum, W. E. A., Maskell, E. C., 1966, “Subsonic Wind Tunnel Wall Corrections,” AGARDograph 109.
- Goethert, B. H., 2007, *Transonic Wind Tunnel Testing*, Dove Publications, Inc., Mineola, New York.
- Goffert, B., Truys, C. F., Lima, D. S. A, Falcão Filho, J. B. P., 2008, “Control of Injection System for the Pilot Transonic Wind Tunnel of IAE in Closed Circuit”, Proceedings ... XII Brazilian Congress of Thermal Engineering and Sciences, ENCIT-2008, Belo Horizonte-MG, article 1-5054.
- Menezes, J. C. L., 1994, “Análise Numérica de Escoamentos Transônicos Turbulentos em Torno de Aerofólio,” Tese de Mestrado, Instituto Tecnológico de Aeronáutica, São José dos Campos – SP.
- PSI, 2000, “ESP-16BP Pressure Scanner User’s Manual,” catalog of products of Esterline Pressure Systems 3<sup>rd</sup> Edition – [www.pressuresystems.com](http://www.pressuresystems.com).
- Testo, 2000, “Instrumentos Portáteis de Medição”, catalog of products of Testo do Brasil Instrumentos de Medição Ltda. – [www.testo.com.br](http://www.testo.com.br).
- Silva, A. F. C., Godinho, M. B. C, Ortega, M. A., Falcão Filho, J. B. P., 2011, “Supersonic/subsonic Mixing Chamber Experimental Analysis”, 21<sup>st</sup> Brazilian Congresso f Mechanical Engineering, COBEM-2011, Natal, RN, Bazil.
- Zucker, R. O., Biblarz, O., 2002, *Fundamentals of Gas Dynamics*, Second Edition, John Wiley & Sons, Inc.

#### 7. RESPONSIBILITY NOTICE

The authors are the only responsible for the printed material included in this paper.